

Effect of microstructure on the electron-phonon interaction in the disordered metals Pd₆₀Ag₄₀

Y. L. Zhong

Department of Physics, National Tsing Hua University, Hsinchu 300, Taiwan

J. J. Lin* and L. Y. Kao

Institute of Physics, National Chiao Tung University, Hsinchu 300, Taiwan

(Received 29 April 2002; published 7 October 2002)

Using the weak-localization method, we have measured the electron-phonon scattering times τ_{ep} in Pd₆₀Ag₄₀ thick films prepared by dc- and rf-sputtering deposition techniques. In both series of samples, we find an anomalous $1/\tau_{ep} \propto T^2 l$ temperature and disorder dependence, where l is the electron elastic mean free path. This anomalous behavior cannot be explained in terms of the current concepts for the electron-phonon interaction in impure conductors. Our result also reveals that the strength of the electron-phonon coupling is much stronger in the dc- than rf-sputtered films, suggesting that the electron-phonon interaction is not only sensitive to the total level of disorder, but is also sensitive to the microscopic quality of the disorder.

DOI: 10.1103/PhysRevB.66.132202

PACS number(s): 72.10.Di, 73.61.At, 72.15.Rn

I. INTRODUCTION

The electron-phonon (e -ph) scattering time τ_{ep} is one of the most important physical quantities in metals and superconductors. For instance, it determines the dephasing (also called the phase-breaking or decoherence) time for the electron wave function, the cooling time for an electron gas, and the relaxation time for the order parameter in a superconductor. The e -ph scattering time also plays a crucial role in the development of novel mesoscopic devices such as sensitive low-temperature bolometers.¹ The e -ph scattering time in the presence of multiple (elastic) impurity scattering has been intensively calculated by several authors,²⁻⁴ but the current understanding of the temperature and electron elastic mean free path, l , dependences of τ_{ep} is still incomplete. In particular, different temperature and disorder dependences of τ_{ep} have been reported, both theoretically and experimentally.^{5,6} Recently, it was proposed that, in addition to the dependence on the total level of disorder, the T and l dependences of τ_{ep} might be fairly sensitive to the microscopic quality of the disorder.⁷⁻⁹ It has also been conjectured that the contribution due to the umklapp process of impurity scattering may be important.¹⁰

In this work, we have fabricated two series of Pd₆₀Ag₄₀ thick films by dc-sputtering and rf-sputtering deposition techniques. The palladium-silver alloys are chosen because Pd and Ag form perfect fcc solid solutions through the alloy series.¹¹ Also, since the masses of the Pd and Ag atoms are quite similar, the vibrational spectrum of the lattice does not change significantly through the alloy series.¹² The low-field magnetoresistances of our films are measured at liquid-helium temperatures and are compared with the weak-localization theoretical predictions to extract the values of the e -ph scattering time. Our results for the temperature and electron mean free path dependences of τ_{ep} and their implications are described below.

II. EXPERIMENTAL METHOD

Our films were prepared from a 99.995% pure Pd₆₀Ag₄₀ (hereafter referred to as PdAg) target. Two series of thick

films were fabricated, one by the dc-sputtering and the other by rf-sputtering deposition technique. The films were deposited onto glass substrates held at room temperature. In both cases, a background pressure of 3×10^{-6} torr was reached before an argon atmosphere of 3.8×10^{-3} torr was introduced to initiate the deposition process. A same sputtering gun was used for these two deposition methods, but with the gun being connected to either a dc or a rf power supply. The distance between the sputtering target and the glass substrates was the same for both methods. The sputtering power was progressively adjusted to “tune” the deposition rate, which resulted in different amounts of disorder, i.e., the residual resistivities $\rho_0 [= \rho(10 \text{ K})]$, in the films. For the dc-sputtering (rf-sputtering) case, the deposition rate was varied from 30 to 230 (19 to 333) Å/min, and values of ρ_0 ranging from 281 to 183 (74 to 178) $\mu\Omega \text{ cm}$ were obtained.

The sample structures of our films were carefully studied by performing the powder diffraction on an MAC MXP18 x-ray diffractometer. The x-ray power was 10 kW and the scanning speed was 6° per minute. In all cases, we found our samples to reveal very similar diffraction patterns, which clearly suggested that both the dc- and rf-sputtered films possessed the same fcc lattice structure characteristic as that of the PdAg alloys. Representative x-ray diffraction patterns for two dc- and two rf-sputtered films are shown in Fig. 1.

Most of our films had a thickness $t \geq 4000$ Å. This thickness ensured that the weak-localization effects were three dimensional in our samples. It also ensured that the thermal phonons were unambiguously three dimensional; i.e., the wavelength of the most probable thermal phonons was always smaller than the film thickness at our measurement temperatures. This latter condition greatly eliminated any complications that might result from phonon confinement effects. (In reduced-dimensional systems, modifications to the phonon spectrum and the speed of sound might be significant, which could lead to nonstraightforward temperature and disorder behavior of τ_{ep} .)

Our values of the diffusion constant D were evaluated through the Einstein relation $\rho_0^{-1} = D e^2 N(0)/(1 + \lambda)$, where $N(0)$ is the electronic density of states at the Fermi level and

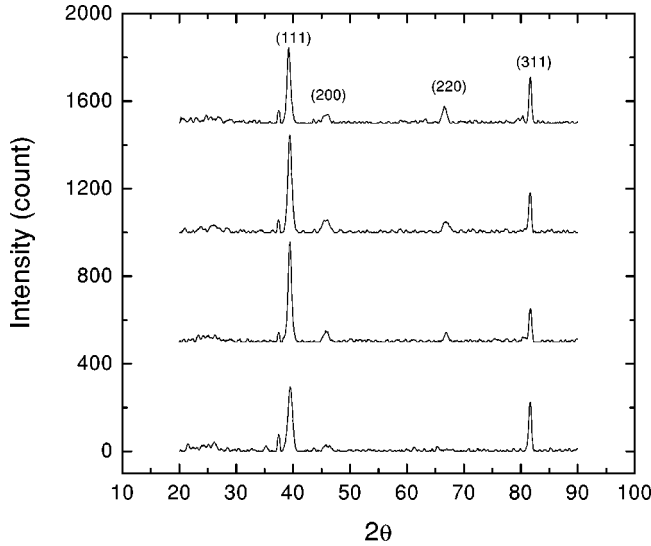


FIG. 1. X-ray diffraction patterns for two dc- (top two curves) and two rf- (bottom two curves) sputtered PdAg thick films. The sample resistivities $\rho(300\text{ K})$ from top down are 189, 82, 79, and $132\ \mu\Omega\text{ cm}$. The diffraction intensity shows an arbitrary unit.

λ is the e -ph mass enhancement factor. The values of $N(0)$ were calculated from the independently determined electronic specific heat: $\gamma T = \frac{1}{3} \pi^2 k_B^2 N(0) T$. For $\text{Pd}_{60}\text{Ag}_{40}$, $\lambda \approx 0.43$ and $\gamma \approx 3.3\text{ mJ/mol K}^2$.¹¹ Then, we obtained $D \approx (100/\rho_0)\text{ cm}^2/\text{s}$, where ρ_0 is in $\mu\Omega\text{ cm}$. Table I lists the values of the relevant parameters for our films studied in this work.

III. RESULTS AND DISCUSSION

The normalized magnetoresistivities $\Delta\rho(B)/\rho^2(0) = [\rho(B) - \rho(0)]/\rho^2(0)$ for the PdAg17 thick film at several temperatures are plotted in Fig. 2. The symbols are the experimental data and the solid curves are the three-dimensional weak-localization theoretical predictions.¹³ It is clearly seen that the weak-localization predictions can de-

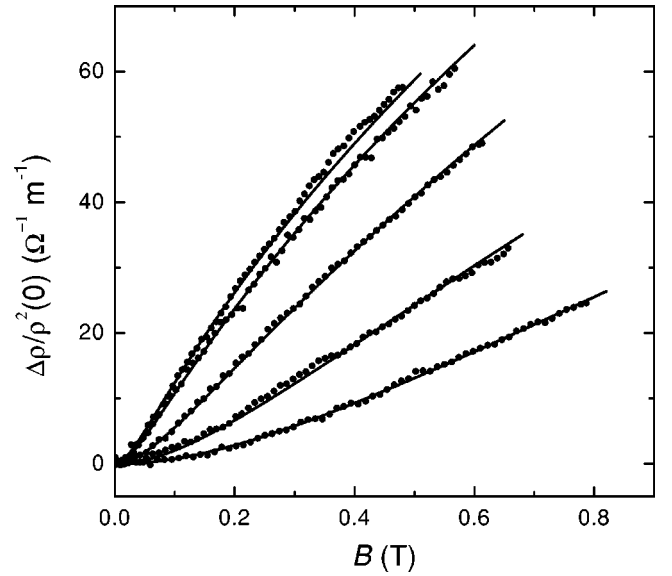


FIG. 2. Normalized magnetoresistivities as a function of magnetic field for the PdAg17 thick film at (from top down) 1.0, 3.0, 6.0, 9.0, and 14.0 K. The solid curves are the three-dimensional weak-localization theoretical predictions.

scribe well our experimental data. Therefore, the electron dephasing time τ_ϕ , which is the key parameter in the weak-localization theory, can be reliably extracted. Since PdAg has a very strong spin-orbit scattering, τ_ϕ is the *only* adjusting parameter in the comparison of the theory with experiment. (That the spin-orbit scattering is strong in PdAg is evident in the shape of the positive magnetoresistivity curves shown in Fig. 2.) The details of our data analysis procedure was discussed previously.¹⁴

In *three* dimensions, the total electron dephasing rate that governs the weak-localization effects is given by¹⁵

$$\frac{1}{\tau_\phi(T, l)} = \frac{1}{\tau_\phi^0(l)} + \frac{1}{\tau_{ep}(T, l)}, \quad (1)$$

TABLE I. Values of the relevant parameters for $\text{Pd}_{60}\text{Ag}_{40}$ thick films. The samples end with (without) a dagger denote films prepared by the dc- (rf-) sputtering deposition technique. t is the film thickness. ρ_0 is the resistivity at 10 K. D is the diffusion coefficient. The values of $k_F l = 3mD/\hbar$ are computed by assuming the free electron mass of m , where k_F is the Fermi wave number. τ_ϕ^0 is the fitted electron dephasing time as $T \rightarrow 0$. A_{ep} and p are the fitted strength of e -ph coupling and effective exponent of temperature, respectively, in $1/\tau_{ep} = A_{ep} T^p$.

Sample	t (Å)	ρ_0 ($\mu\Omega\text{ cm}$)	D (cm^2/s)	$k_F l$	τ_ϕ^0 (10^{-10} s)	A_{ep} ($10^8\text{ s}^{-1}\text{ K}^{-p}$)	p
PdAg11 [†]	3900	281	0.36	0.93	2.8	1.5	2.3 ± 0.1
PdAg15 [†]	5100	235	0.43	1.1	1.1	2.4	1.9 ± 0.2
PdAg08 [†]	3900	224	0.45	1.2	6.7	2.0	2.4 ± 0.1
PdAg12 [†]	4800	183	0.55	1.4	3.7	2.8	2.2 ± 0.1
PdAg18	5000	178	0.56	1.5	4.3	0.40	2.4 ± 0.1
PdAg17	4500	101	0.99	2.6	1.6	2.2	2.2 ± 0.1
PdAg19	4000	98	1.0	2.6	1.6	2.9	2.3 ± 0.1
PdAg14	4100	90	1.1	2.9	1.1	2.5	2.2 ± 0.2
PdAg16	3300	74	1.3	3.5	0.97	3.6	2.2 ± 0.1

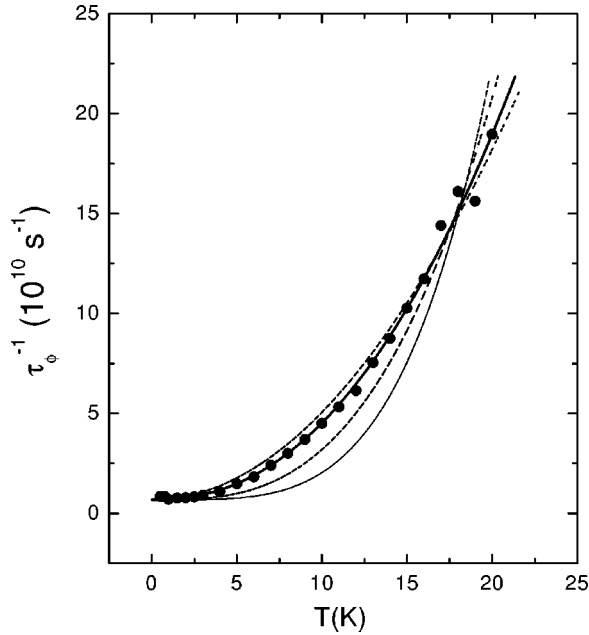


FIG. 3. Electron dephasing rate as a function of temperature for the PdAg17 thick film. The thick solid curve drawn through the data points is a least-squares fit to Eq. (1), using p as a free parameter. The dotted, dashed, and thin solid curves are least-squares fits to Eq. (1) with p fixed at 2, 3, and 4, respectively (see text).

where $\tau_\phi^0 = \tau_\phi(T \rightarrow 0)$ depends very weakly on temperature, if at all, and is called the saturated dephasing time. Whether τ_ϕ^0 should reach a finite or an infinite value as $T \rightarrow 0$ is currently under vigorous experimental and theoretical investigations.⁶ At finite temperatures, the dominating inelastic electron process in three dimensions is solely due to the e -ph scattering, while the Nyquist electron-electron scattering is negligibly small.^{6,15,16} Usually, one writes $1/\tau_{ep} = A_{ep} T^p$ over the limited temperature range accessible in a typical experiment, where A_{ep} characterizes the strength of the e -ph coupling and p is an effective exponent of temperature. According to current understanding, p lies between 2 and 4.^{2-4,9}

The extracted $\tau_\phi(T)$ between 0.5 and 20 K for each of our films is least-squares fitted to Eq. (1), and the fitted values of the relevant parameters (τ_ϕ^0 , A_{ep} , and p) are listed in Table I. Figure 3 shows a plot of the variation of $1/\tau_\phi$ with temperature for the PdAg17 thick film. The symbols are the experimental data. The thick solid curve drawn through the data points is obtained with τ_ϕ^0 , A_{ep} , and p as free parameters. In this case, we obtain a temperature exponent $p = 2.2 \pm 0.1$. For comparison, we have also least-squares fitted the measured $1/\tau_\phi$ with Eq. (1), but with p fixed at an integer value of either 2, 3, or 4 (while allowing τ_ϕ^0 and A_{ep} to vary). The dotted, dashed, and thin solid curves in Fig. 3 plot the fitted results with $p=2$, 3, and 4, respectively. It is clearly seen that our temperature dependence of $1/\tau_{ep}$ can be best described with an exponent p equal or close to 2. In fact, we have found that the temperature behavior of τ_{ep} for all films listed in Table I is very similar; i.e., $1/\tau_{ep}$ demonstrates an *essentially quadratic* temperature dependence.

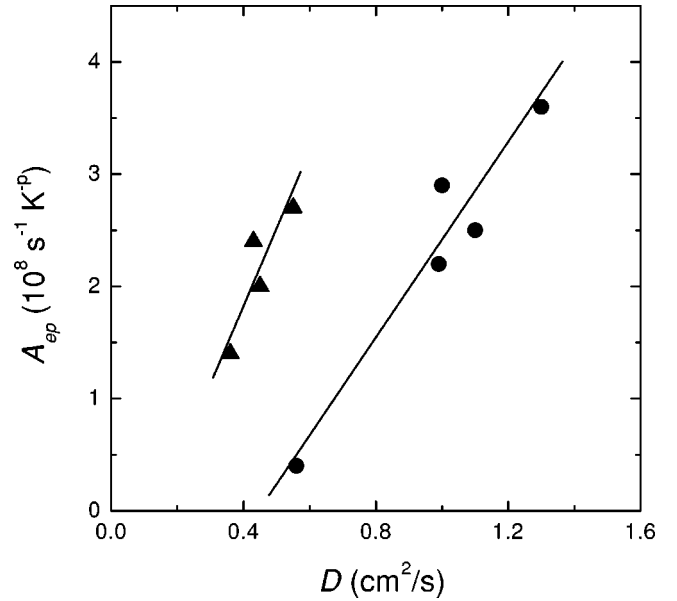


FIG. 4. The strength of e -ph coupling A_{ep} as a function of diffusion constant for dc- (triangles) and rf- (circles) sputtered PdAg thick films. The straight lines drawn through the data points are guides to the eye.

Inspection of Table I indicates that, for either dc- or rf-sputtered films, the value of A_{ep} decreases with increasing level of disorder (ρ_0) in the sample. Figure 4 plots the fitted A_{ep} as a function of the diffusion constant. Clearly, one sees that A_{ep} varies *linearly* with D , implying that $1/\tau_{ep} \propto D \propto l$. It should be noted that, if we plot $1/\tau_{ep}$ as a function of the measured ρ_0^{-1} , we also observe a linear variation, i.e., $1/\tau_{ep} \propto \rho_0^{-1} \propto l$. Such a linearity of A_{ep} with l holds for *both* series of films. Quantitatively, however, the values of A_{ep} (for a given disorder) for the dc- and rf-sputtered films are very different. For example, while the dc-sputtered PdAg12 and the rf-sputtered PdAg18 thick films have essentially the same ρ_0 , their values of A_{ep} differ by several times. Moreover, Fig. 4 reveals that the slope of the linearity is about a factor of 2 larger in the dc- than rf-sputtered films. Since the x-ray diffraction studies demonstrate that the crystal structures are quite similar for both series of films (Fig. 1), the differences in the values of A_{ep} and the variation of A_{ep} with l strongly imply that the e -ph interaction must be very sensitive to the microstructures of the samples. The subtle difference in the microstructures in these two series of films may result from the different ways of sample preparation.

Taken together, Figs. 3 and 4 demonstrate that the e -ph scattering in PdAg possesses an *anomalous* temperature and disorder dependence of $1/\tau_{ep} \propto T^2 l$. This dependence is insensitive to the fabrication method. Such a $T^2 l$ behavior is totally unexpected, even qualitatively, in terms of the current theoretical concepts for the e -ph interaction in impure conductors. According to the “orthodox” e -ph interaction theory for disordered metals,²⁻⁴ which assumes a coherent motion of impurity atoms with deformed lattice atoms at low temperatures, one should expect a $T^4 l$ dependence. Recently, it was speculated that, in real metals containing heavy (light) impurities and tough boundaries, the impurity and/or bound-

ary atoms might not move in phase with the lattice atoms.⁷ The first calculations in consideration of this effect have been done by Sergeev and Mitin.⁹ They found that even a small amount of “static” potential scatterers drastically changes the e -ph-impurity interference, and the relaxation rate is proportional to $T^2\mathcal{L}^{-1}$, where \mathcal{L} is the electron mean free path with respect to the static impurities ($\mathcal{L}\gg l$). Experimentally, a T^4 temperature dependence has been observed very recently in disordered Hf and Ti thin films.¹ (A T^4 dependence had been previously observed in Bi thin films over a very limited temperature range of 0.6–1.2 K.¹⁷) However, to the best of the authors’ knowledge, the combined T^4l law has never been confirmed in real conductors thus far. On the other hand, a distinct T^2l^{-1} dependence has been observed in $\text{Ti}_{1-x}\text{Al}_x$ (Ref. 7) and $\text{Ti}_{1-x}\text{Sn}_x$ (Ref. 8) alloys. Previously, a T^2l dependence was independently found in AuPd thick films¹⁵ ($t\gtrsim 4000$ Å), and Nb thin films¹⁸ ($t\lesssim 200$ Å). In the present case of PdAg thick films, the masses of the Pd and Ag atoms are quite similar, and the films are three dimensional. Therefore, it is not clear how the Sergeev-Mitin theory evoking heavy (light) impurities and tough boundaries can apply to this case.

The criterion for the e -ph interaction to satisfy the dirty-limit condition is $q_Tl\ll 1$, where the wave number of the thermal phonons $q_T\approx k_B T/\hbar v_s$ and v_s is the speed of sound. Taking $v_s\approx 2600$ m/s (Ref. 19) and $l\approx 2-8$ Å, we obtain

$q_T T\approx (0.01-0.04)T$ for our PdAg thick films. The phase-breaking lengths $\sqrt{D\tau_\phi}$ in our films are calculated to be 690–1500 Å at 2 K. (The dephasing length essentially saturates below about 2 K.) This length scale justifies the use of three-dimensional weak-localization theory to describe our experimental magnetoresistivities.

IV. CONCLUSION

We have measured the e -ph scattering time τ_{ep} in dc- and rf-sputtered PdAg thick films. In both series of films, we observe an anomalous $1/\tau_{ep}\propto T^2l$ temperature and disorder dependence. Moreover, the e -ph coupling is found to be much stronger in the dc- than rf-sputtered films. This observation strongly indicates that the e -ph interaction is not only sensitive to the total level of disorder, but is also sensitive to the microscopic quality of the disorder. These results pose a new theoretical challenge.

ACKNOWLEDGMENTS

We are grateful to V. Mitin, A. Sergeev, and G. Y. Wu for valuable discussions. This work was supported by the Taiwan National Science Council through Grant Nos. NSC90-2112-M-009-037 and NSC90-2119-M-007-004.

*Electronic address: jjlin@cc.nctu.edu.tw

¹M.E. Gershenson, D. Gong, T. Sato, B.S. Karasik, and A.V. Sergeev, Appl. Phys. Lett. **79**, 2049 (2001).

²J. Rammer and A. Schmid, Phys. Rev. B **34**, 1352 (1986).

³M.Yu Reizer and A.V. Sergeyev, Zh. Éksp. Teor. Fiz. **90**, 1056 (1986) [Sov. Phys. JETP **63**, 616 (1986)].

⁴D. Belitz, Phys. Rev. B **36**, 2513 (1987).

⁵J.J. Lin, Physica B **279**, 191 (2000).

⁶See, for a recent review, J.J. Lin and J.P. Bird, J. Phys.: Condens. Matter **14**, R501 (2002).

⁷J.J. Lin and C.Y. Wu, Europhys. Lett. **29**, 141 (1995).

⁸C.Y. Wu, W.B. Jian, and J.J. Lin, Phys. Rev. B **57**, 11 232 (1998).

⁹A. Sergeev and V. Mitin, Phys. Rev. B **61**, 6041 (2000); Europhys. Lett. **51**, 641 (2000).

¹⁰W. Jan, G.Y. Wu, and H.S. Wei, Phys. Rev. B **64**, 165101 (2001); W. Jan and G.Y. Wu, J. Phys.: Condens. Matter **13**, 10925 (2001).

¹¹P.M. Laufer and D.A. Papaconstantopoulos, Phys. Rev. B **35**, 9019 (1987).

¹²J.S. Dugdale, *The Electrical Properties of Metals and Alloys* (Edward Arnold, London, 1977).

¹³H. Fukuyama and K. Hoshino, J. Phys. Soc. Jpn. **50**, 2131 (1981).

¹⁴C.Y. Wu and J.J. Lin, Phys. Rev. B **50**, 385 (1994).

¹⁵Y.L. Zhong and J.J. Lin, Phys. Rev. Lett. **80**, 588 (1998).

¹⁶M.E. Gershenson, Ann. Phys. (Leipzig) **8**, 559 (1999).

¹⁷Yu.F. Komnik, V.Yu. Kashirin, B.I. Belevtsev, and E.Yu. Beliaev, Phys. Rev. B **50**, 15 298 (1994).

¹⁸E.M. Gershenson, M.E. Gershenson, G.N. Gol’tsman, A.M. Lyul’kin, A.D. Semenov, and A.V. Sergeev, Zh. Éksp. Teor. Fiz. **97**, 901 (1990) [Sov. Phys. JETP **70**, 505 (1990)].

¹⁹*The Practicing Scientist’s Handbook*, edited by A. J. Moses (Van Nostrand Reinhold, New York, 1978); W.C. McGinnis and P.M. Chaikin, Phys. Rev. B **32**, 6319 (1985).